Proc. Natl. Acad. Sci. USA
Vol. 94, pp. 12932–12937, November 1997
Cell Biology

Phagocytosis of rod outer segments by retinal pigment epithelial cells requires αvβ5 integrin for binding but not for internalization

SILVIA C. FINNEMANN, VERA L. BONILHA, ALAN D. MARMORSTEIN, AND ENRIQUE RODRIGUEZ-BOULAN

Margaret M. Dyson Vision Research Institute, Department of Ophthalmology, and Department of Cell Biology, Cornell University Medical College, New York, NY 10021

Communicated by Torsten N. Wiesel, Rockefeller University, New York, NY, October 3, 1997 (received for review July 1, 1997)

ABSTRACT **Phagocytosis of shed photoreceptor rod outer segments (ROS) by the retinal pigment epithelium (RPE) is essential for retinal function. Here, we demonstrate that this process requires αvβ5 integrin, rather than αvβ3 integrin utilized by systemic macrophages. Although adult rat RPE expressed both αvβ3 and αvβ5 integrins, only αvβ3 was expressed at birth, when the retina is immature and phagocytosis is absent. Expression of αvβ5 was first detected in RPE at PN7 and reached adult levels at PN11, just before onset of phagocytic activity. Interestingly, αvβ5 localized *in vivo* to the apical plasma membrane, facing the photoreceptors, and to intracellular vesicles, whereas αvβ3 was expressed basolaterally. Using quantitative fluorimaging to assess *in vitro* uptake of fluorescent particles by human (ARPE-19) and rat (RPE-J) cell lines, αvβ5 function-blocking antibodies were shown to reduce phagocytosis by drastically decreasing (85%) binding of ROS but not of latex beads. In agreement with a role for αvβ5 in phagocytosis, immunofluorescence experiments demonstrated codistribution of αvβ5 integrin with internalized ROS. Control experiments showed that blocking αvβ3 function with antibodies did not inhibit ROS phagocytosis and that αvβ3 did not colocalize with phagocytosed ROS. Taken together, our results indicate that the RPE requires the integrin receptor αvβ5 specifically for the binding of ROS and that phagocytosis involves internalization of a ROS-αvβ5 complex. αvβ5 integrin does not participate in phagocytosis by other phagocytic cells and is the first of the RPE receptors involved in ROS phagocytosis that may be specific for this process.**

Among the vital functions performed by the retinal pigment epithelium (RPE) (1) is the phagocytosis of rod outer segments (ROS) fragments (2). At birth, rat RPE cells lack phagocytic ability (3, 4). During postnatal retinal maturation, the RPE forms long, apical microvilli that ensheath developing photoreceptor outer segments. From about PN12, stacks of ROS membranes are shed daily from the distal end of photoreceptors and become efficiently phagocytosed by RPE cells (5). The essential role of RPE phagocytosis is highlighted by the rapid degeneration of photoreceptor neurons in Royal College of Surgeons rats. Royal College of Surgeons rats carry an autosomal recessive mutation that impairs RPE phagocytosis, resulting in subretinal accumulation of ROS (3, 6, 7). Photoreceptor death is irreversible and inevitably results in blindness (8, 9).

RPE phagocytosis is poorly understood, compared with the well characterized phagocytosis by monocyte macrophages. RPE and systemic phagocytosis differ in that the former follows a circadian rhythm in many species (10). Furthermore, although RPE cells express Fc receptors, they highly favor ROS binding and uptake over internalization of opsonized bacteria, yeast or inert particles (11). Of special relevance to RPE phagocytosis is the phagocytosis of apoptotic cells by circulating macrophages. Clearance of senescent cells by monocyte macrophages requires two macrophage surface receptors: the scavenger receptor CD36/thrombospondin receptor and the integrin αvβ3, bridged by soluble thrombospondin (12, 13). Although the ligand for this cluster has yet to be identified, CD36 may bind individually anionic phospholipids on the apoptotic cell surface, triggering a parallel, αvβ3-independent phagocytic pathway (14).

Some of the receptors involved in systemic phagocytosis have been reported to participate in RPE phagocytosis of ROS. Indirect evidence involves a mannose receptor in ROS phagocytosis, but neither the RPE receptor nor the ligand on the surface of ROS have been identified (15, 16). More recent work has shown that CD36 is present in the RPE and, when transfected into melanoma cells, confers the ability to phagocytose ROS (17). Furthermore, *in vitro* experiments show that anionic phospholipids and CD36 antibodies partially inhibit ROS phagocytosis by RPE cells (18). However, RPE cells do not take up ROS via the CD36/αvβ3/thrombospondin dependent phagocytic pathway, raising the possibility that alternative RPE molecules cooperate with CD36 in the uptake of ROS. Recently, Hall *et al.* (19) employed an antiserum that interferes with ROS binding to RPE cells to isolate RPE molecules involved in phagocytosis. They obtained partial peptide sequences of seven RPE surface antigens, one of which revealed homology to an integrin subunit. The presence of integrins at the RPE-photoreceptor interface was reported but their function was not identified (20).

In this report, we show that the vitronectin receptor αvβ5 is expressed by the RPE of newborn rats just before the onset of ROS phagocytosis. We utilize a sensitive and quantitative *in vitro* assay and immunofluorescence data to provide compelling evidence for the involvement of this integrin in an early step of RPE phagocytosis.

MATERIALS AND METHODS

Reagents. Unless otherwise indicated, reagents were obtained from Sigma or Life Technologies (Grand Island, NY).

Antibodies. αv integrin antiserum was a gift from F. Giancotti (New York University, New York). β3 integrin antibody F11 was provided by M. H. Helfrich (Imperial Cancer Research Fund, London) (21). β5 and αvβ3 LM609 (22) antibodies were from Chemicon. β3 integrin antibody was from Transduction Laboratories (Lexington, KY). β1 integrin and vitronectin receptor antisera and inhibiting mAb against αvβ5 integrin PIF6 (23) were from GIBCO. H4 αvβ3 mAb was from BioSource International (Camarillo, CA).

Cell Culture, Animals, and Tissue Preparation. RPE-J and ARPE-19 cells were cultured and differentiated on 6.5 mm

The publication costs of this article were defrayed in part by page charge payment. This article must therefore be hereby marked "*advertisement*" in accordance with 18 U.S.C. §1734 solely to indicate this fact.

Abbreviations: RPE, retinal pigment epithelium; ROS, rod outer segments; FITC, fluorescein isothiocyanate.

diameter Transwell filters (Corning-Costar) as described previously (24, 25). Long Evans rats (Harlan Breeders, Indianapolis) were sacrificed at various ages by CO_2 asphyxiation. For biochemistry, RPE was prepared from enucleated eyes according to established protocols (26). ROS were isolated from fresh bovine eyes obtained from the slaughterhouse as described earlier (27). ROS were stored suspended in 10 mM Na-phosphate (pH 7.2), 0.1 M NaCl, and 2.5% sucrose at −80°C. Before use, ROS were labeled in 1 mg/ml fluorescein isothiocyanate (FITC) or Texas red (both Molecular Probes) in 0.1 M Na-bicarbonate (pH 9.0), for 1 h in the dark, before being washed and resuspended in cell culture medium with 2.5% sucrose at 5×10^7 ROS/ml.

Phagocytosis Assays and ROS Quantification. Unlabeled or fluorescent ROS (2×10^6) were added in 50 μl of the respective culture medium containing 2.5% sucrose (11) to the apical surface of differentiated RPE-J or ARPE-19 cells. For inhibition studies, cells were preincubated with antibody and/or peptide diluted in culture medium for 30 min and fresh inhibiting reagent was added with ROS. Phagocytosis was allowed for various lengths of time under the respective culture conditions or on ice before rinsing filters four times with PBS containing 1 mM $MgCl_2$ and 0.2 mM $CaCl_2$ (PBS-CM). To quench external FITC fluorescence, samples were incubated with 0.2% trypan blue in PBS-CM for 10 min prior to fixation (28). Cells were fixed by incubation in ice cold methanol for 5 min followed by incubation in 3% paraformaldehyde in PBS-CM for 10 min at room temperature. Samples were washed extensively in PBS-CM and incubated with 2.5 μg/ml DNAse-free RNAse (Boehringer Mannheim) in PBS-CM for 30 min. Nuclei were stained with 1 μg/ml propidium iodide (Molecular Probes) in PBS-CM for 20 min before samples were mounted in Vectashield (Vector Laboratories). For quantification of FITC-fluorescence emission, samples were scanned with a STORM 860 imager, at 950 V (blue fluorescence) (Molecular Dynamics). Images were processed with Imagequant 1.1 (Molecular Dynamics) and intensities calculated with Excel 5.0. In some cases, samples were scanned after phagocytosis to measure total fluorescence, then treated with trypan blue, fixed, and rescanned, to determine the internalized ROS fraction in the same sample. Labeled samples were also observed with a laser scanning confocal microscope (Sarastro/Molecular Dynamics).

Double Immunofluorescence Labeling of Phagocytosed ROS. RPE cells were fixed in 3% paraformaldehyde after phagocytosis followed by double immunofluorescence staining as previously described (29) using rhodopsin mAb to recognize ROS. Secondary antibodies conjugated to either Cy3 or FITC (both Jackson ImmunoResearch) were used for the labeling before and after permeabilization, respectively. Reversal of secondary antibodies yielded identical results. Samples were mounted and evaluated as described above.

Immunofluorescence Labeling of Tissue Cryosections or Cells. Retinas of isolated eyecups were enzymatically removed (26). These samples were fixed in ice cold methanol or 3% paraformaldehyde, rehydrated in PBS-CM, infused with 30% sucrose in PBS-CM, embedded in OCT (Miles). Transverse sections (10 μm) of eyecups were cut and immunolabeled. Differentiated monolayers of RPE cells were fixed in ice cold methanol (for β5 integrin staining) or 3% paraformaldehyde in PBS-CM for 30 min and reequilibrated in PBS-CM. Immunofluorescence staining was performed as described (26).

Sample Lysis, SDS/PAGE, and Immunoblotting. Tissue samples or cells on filters were lysed in PBS-CM supplemented with 1% each of Triton X-100 and Nonidet P-40; 2 mM each of aprotinin, leupeptin, pepstatin, iodoacetamide, and phenylmethylsulfonyl fluoride; and 1 mM *N*-ethylmaleimide. Protein concentration was determined and equal amounts subjected to nonreducing 7.5% SDS/PAGE followed by Western blot detection of integrins as published previously (30).

RESULTS

We examined the expression and subcellular distribution of integrins in the adult rat RPE. Immunofluorescence staining of fibronectin receptors with a generic antibody against β1 heterodimers (Fig. 1*A*, $\alpha x\beta 1$), or with antibodies against the predominant β1 partners in the RPE, α3 or α6 (data not shown), demonstrated basolateral localization in all cases. In contrast, generic staining of vitronectin receptors with antibodies against αv heterodimers or the αv subunit (Fig. 1*A*, $\alpha v\beta x$ and αv) detected staining on both apical and basolateral

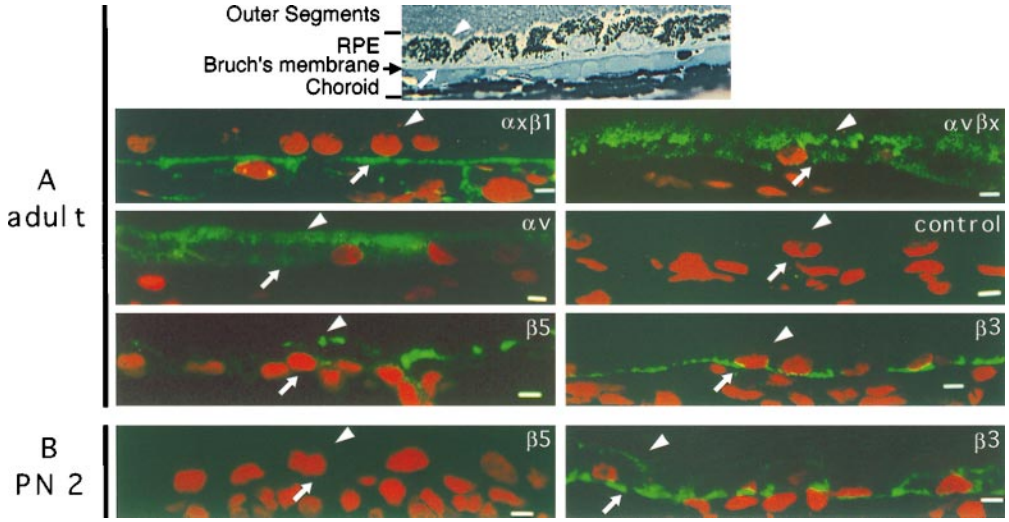

FIG. 1. β5 integrin is expressed apically by the adult RPE but is not expressed at PN2. For reference, a methylene blue stained thick section with intact retina is shown at the top. Adult rat RPE: The subcellular distribution of integrin receptors or their subunits was determined on cryosections of adult rat eyes by indirect immunofluorescence. While β1 integrin receptors were exclusively basal (*A*, $\alpha x\beta 1$), αv integrin receptors were localized on both apical and basolateral surface, as well an on cytoplasmic vesicles (*A*, $\alpha v\beta x$). The αv subunit stained cytoplasm and all plasma membrane domains. Nonspecific IgG gave only background staining (*A*, control). The β5 integrin was detected only apically in the adult RPE (*A*, β5) while β3 integrin was restricted basally (*A*, β3). Note that β5 antibody immunostaining required methanol fixation after removal of the neural retina causing occasional disruption of the apical RPE surface. Immature rat RPE: at PN2 (*B*) β5 integrin was not detected (*B*, β5). In contrast, β3 integrin was expressed with a nonpolar distribution (*B*, β3). (Bars = 5 μm.)

domains and in cytoplasmic vesicles. Apparent larger amounts of cytoplasmic αv subunits than αv containing receptors may indicate undimerized αv protein in RPE cells. Staining with β3 and β5 subunit-specific antibodies demonstrated that this distribution was explained by the complementary, nonoverlapping distributions of two vitronectin receptors, αvβ3 on the basolateral membrane and αvβ5 on the apical surface and in cytoplasmic vesicles (Fig. 1*A*, β3 and β5). An important conclusion of this experiment is that, of all integrins expressed in the rat RPE, only αvβ5 displayed the apical and vesicular localization expected of a protein involved in ROS phagocytosis.

A protein involved in ROS phagocytosis might not be needed before the onset of this process, which occurs two weeks after birth in the rat (see *Introduction*). Immunofluorescence experiments indicated that the RPE from 2 days old rats expresses β3 (Fig. 1*B*, β3), but no β5 (Fig. 1*B*, β5). In agreement with these results, immunoblots of RPE lysates from newborn rats detected adult levels of β3 and αv as early as PN2 but detected no β5 at PN2, low levels at PN7 and adult RPE levels of this protein after PN11 (Fig. 2*A*).

To test directly the involvement of αvβ3 and αvβ5 integrins in ROS phagocytosis, we modified a standard *in vitro* fluorescent ROS phagocytosis assay, originally established for primary cultures of RPE (29). In our experiments, we studied a human (ARPE-19) and a rat (RPE-J) RPE cell line, which retain many characteristics of cultured primary RPE cells (24, 25). Comparative immunoblots confirmed that both cell lines express αv, β3, and β5 subunits at similar levels as adult rat RPE (Fig. 2 *A–C*). The kinetics of ROS phagocytosis by confluent monolayers of RPE-J cells is shown in Figs. 3 and 4. Increasing levels of FITC-ROS associated with the cells after 2 h and 5 h at 39°C, but only background levels were observed after 2 h at 0°C (Fig. 3 *A, D, G*). This established that the RPE-J cell line was capable of receptor-mediated ROS phagocytosis, and so were ARPE-19 cells (data not shown). Trypan blue quenching after the 2 h incubation abolished FITC-

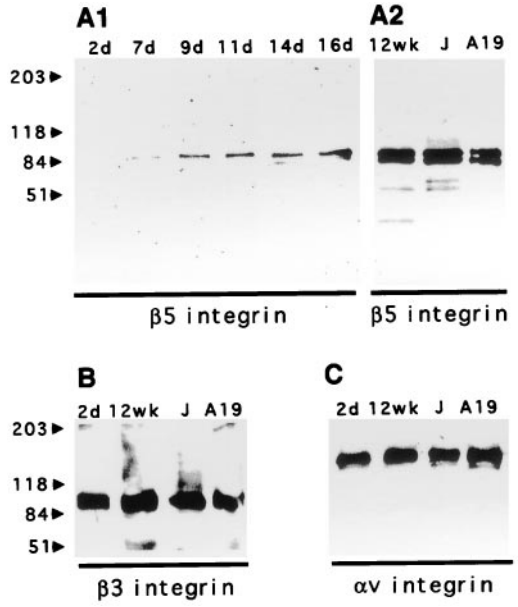

FIG. 2. Immunoblot detects β5 integrin expression after PN7, whereas αv and β3 are expressed at constant adult levels from birth. In RPE obtained from rats of various ages, β5 integrin was first detected at PN7 but acquired its adult expression level only at PN11 (*A1*, 10 μg protein per lane, *A2*, 50 μg per lane). β3 and αv integrins were expressed at adult levels from PN2 (*B* and *C*, 50 μg per lane). RPE-J (J) and ARPE-19 (A19) cell lines displayed similar integrin expression levels as adult RPE (*A2, B, C*, 50 μg per lane). Molecular mass standards are indicated in kDa.

fluorescence, indicating that most of the phagocytosed ROS were extracellular at this time; in contrast, a large fraction of FITC-ROS was internalized after 5 h of continuous exposure to ROS (Fig. 3 *B, E, H*). Parallel experiments in which extracellular ROS were identified by the accessibility of rhodopsin to indirect immuno-labeling before and after RPE permeabilization (Fig. 3 *C, F, I*) confirmed these results.

The uptake of FITC-ROS by RPE-J and ARPE-19 monolayers was quantified using sensitive fluorescence imaging (see *Methods*). The results were identical with both cell lines; hence only RPE-J data are shown (Fig. 4). After a 1 h lag, uptake of FITC-ROS occurred rapidly between 1–3 h (reaching 12-fold over background, 81% of total uptake) and slowed down between 3–5 h (19% of total uptake). Practically all FITC-ROS uptake after 2 h was quenched by trypan blue, confirming the immunofluorescence data in Fig. 3. Between 2–5 h, the internalized fraction of FITC-ROS uptake increased linearly to 5.3-fold over background uptake levels (53% of total uptake). Addition of blocking antibodies to αvβ5 integrin 30 min before ROS challenge drastically inhibited FITC-ROS uptake after 2 h (by 84%) but the inhibition was mostly overcome at later time points (19% at 5 h) (see *Discussion*). FITC-labeled latex beads were bound and internalized by RPE-J or ARPE-19 cells with no lag phase and no inhibition by αvβ5 antibody (data not shown).

Fig. 5*A* characterizes the inhibition of FITC-ROS uptake after 2 h by antibodies or ligands that block integrin function. Inhibition by αvβ5 antibody was 13% at 10 μg/ml, 31% at 25 μg/ml and 84% at 50 μg/ml. Higher antibody concentrations of 100 and 200 μg/ml inhibited to the same degree (data not shown). Thus, αvβ5 antibody inhibition was saturated at 50 μg/ml and this concentration was chosen for all further experiments. Neither nonspecific murine IgG nor fibronectin receptor antiserum (data not shown) decreased ROS uptake. Importantly, none of three mAbs to αvβ3 receptor inhibited ROS uptake (Fig. 5*A*). Since αvβ5 binding to its cognate ligand, vitronectin, requires an RGD site (31), we tested the effect of an RGD containing peptide on ROS uptake. We observed a 52% inhibition by the peptide GRGDSP that was not observed in the presence of the control peptide GRADSP. Interestingly, vitronectin, added in an equivalent molar amount as the RGD peptide, was not inhibitory, suggesting that the ligand on the ROS surface recognized by αvβ5 is distinct from vitronectin.

The kinetics of antibody inhibition, with a maximum effect at 2 h followed by a progressively smaller effect (Fig. 4), suggested that αvβ5 was involved in an early step in phagocytosis, possibly binding. To determine whether the antibody affected internalization, we carried out the experiment shown in Fig. 5*B*. RPE cells were challenged with ROS in the presence or absence of αvβ5 antibodies for 2 h; unbound ROS were then removed and the incubation continued either in the absence or in the presence of inhibitory antibody (Fig. 5*B*, scheme). During the initial stage (0–2 h), uptake of ROS in the presence of 50 μg/ml antibody was 16% of control, as shown above. At the end of the second stage (2–5 h), the internalized fraction of ROS was assessed for each of the four experimental conditions. The results are represented by a bar graph in Fig. 5*B*. Strikingly, RPE cells internalized about 80% of ROS that were bound during the initial 2 h in all cases, independently of the presence or absence of antibody in the second phase. The drastic inhibition of ROS uptake in the first 2 h and the lack of effect of αvβ5 antibody on the internalization between 2–5 h of prebound ROS indicate that αvβ5 participates only in the earlier phase of ROS phagocytosis.

Fig. 4 shows that prolonged times of ROS challenge resulted in an increase in internalized ROS without a proportional increase in the total amount of ROS. This suggests that binding of new ROS declines with time even when large amounts of ROS are available. To test whether the decline in binding might be caused by the depletion of αvβ5 through its inter-

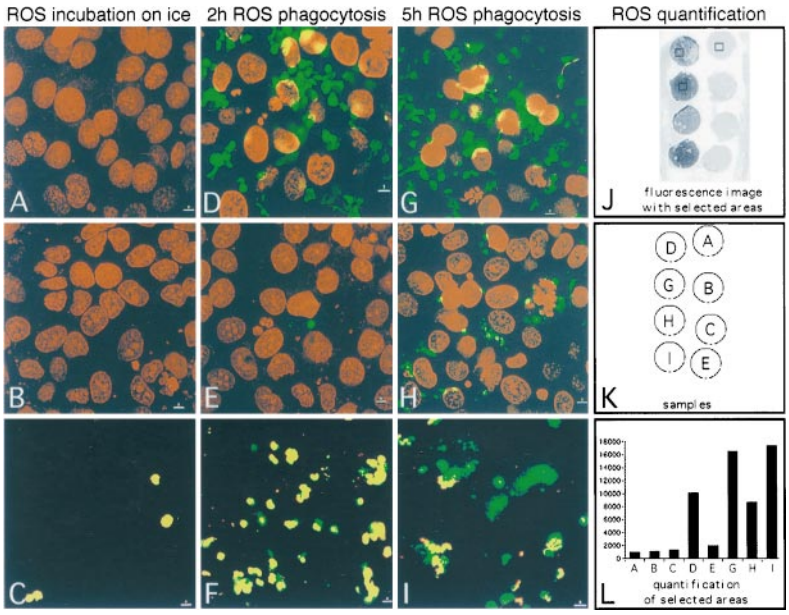

FIG. 3. Laser scanning confocal microscopy and quantitative fluorescence imaging of FITC-ROS phagocytosis by RPE-J cells. (*A, B, D, E, G, H*) Confluent RPE-J monolayers were challenged with FITC-ROS for 2 or 5 h, fixed, and nuclei were stained with propidium iodide. (*B, E, H*) fluorescence of extracellular ROS was quenched with trypan blue. (*C, F, I*) RPE-J cells were challenged with unlabeled ROS for 2 or 5 h, fixed, and rhodopsin stained with Cy3 secondary antibody before permeabilization and with FITC secondary antibody after permeabilization. ROS accessible for labeling before permeabilization appear in yellow due to double staining, while internalized ROS appear in green. Note that after 5 h of phagocytosis, some internalized ROS have been lysed as indicated by a dispersed intracellular fluorescence. (*J–L*) Fluorescence imaging quantification. The same filter used to obtain the confocal images were used for quantification (*K*). Representative fields of constant areas (rectangles in *J*) were scanned; fluorescence intensities are shown as bar graph in *L*. Fluorescence derived from FITC-ROS and immunolabeled ROS were within 10% of each other. (Bars = 5 μm.)

nalization with phagocytosed ROS, we immunolabeled β5 or β3 integrin using FITC secondary antibodies in RPE-J cells that had been exposed to Texas Red labeled ROS for 5 h. x-y confocal sections taken at the level of the nuclei detected comparable diffuse levels of β5 and β3 immunofluorescence in control RPE-J cells (Fig. 6 *A* and *C*). After 5 h ROS challenge, $\alpha v\beta$5 integrin was found in vesicular structures in the cytoplasm that were loaded with ROS, whereas the β3 integrin distribution remained diffuse (Fig. 6 *B* and *D*). These results demonstrate that β5 integrin is specifically relocalized to cytoplasmic compartments containing internalized ROS.

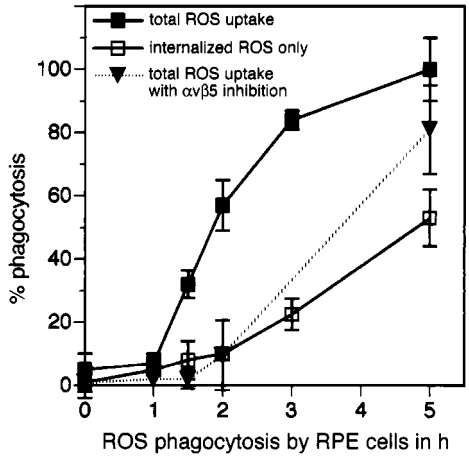

FIG. 4. Time course of ROS phagocytosis by RPE-J cells; inhibition by $\alpha v\beta$5 antibody. Internalized fluorescence of samples was measured after trypan blue quenching of extracellular fluorescence. All samples are expressed as percent of total fluorescence after 5 h phagocytosis, which is taken as 100%. Note that practically all fluorescence was extracellular at time points up to 2 h of ROS challenge. In the presence of $\alpha v\beta$5 blocking antibody, total phagocytosis was reduced at all time points (▼), but most intensely at 2 h. Values represent mean ± SD, $n = 8$.

DISCUSSION

Here, we utilize two stable, clonal, polarized RPE cell lines that retain the ability of the native epithelium to phagocytose ROS, to study the role of integrin receptors in this process. The use of these cell lines greatly facilitates the study of RPE phagocytosis because of their unlimited availability, and the reduced need for animals as a source of RPE. Like native RPE cells, both cell lines take up ROS using a specific receptor-mediated mechanism; furthermore, they display the integrin receptor profile of native RPE cells and express morphological and biochemical features of the native epithelium. The easy access to large numbers of cells allowed us to develop a sensitive and precise fluorimager assay that typically measures uptake of fluorescent ROS by a sample of 2×10^5 cells forming a polarized confluent monolayer on a semipermeable filter. We took advantage of the previously described ability of trypan blue to selectively quench extracellular fluorescence to quantitatively discriminate binding and internalization fractions of the uptake process.

We found that ROS phagocytosis differed from monocyte phagocytosis in that it utilizes the $\alpha v\beta$5 integrin receptor, instead of the $\alpha v\beta$3 integrin receptor. Both $\alpha v\beta$3 and $\alpha v\beta$5 bind vitronectin, but the two integrins differ strikingly in the cytoplasmic signaling pathways that they trigger upon ligand binding (32, 33). Expression of $\alpha v\beta$5 integrin in newborn rat RPE cells correlated temporally and spatially with the onset of phagocytic activity; inhibition of $\alpha v\beta$5 integrin function reduced ROS binding to the RPE surface by 84%. Additional experiments indicated that $\alpha v\beta$5 integrin is involved only in an initial step of phagocytosis. The major inhibitory activity of $\alpha v\beta$5 antibody was observed when the antibody was added prior to the challenge with ROS and kept for the 2 initial hours

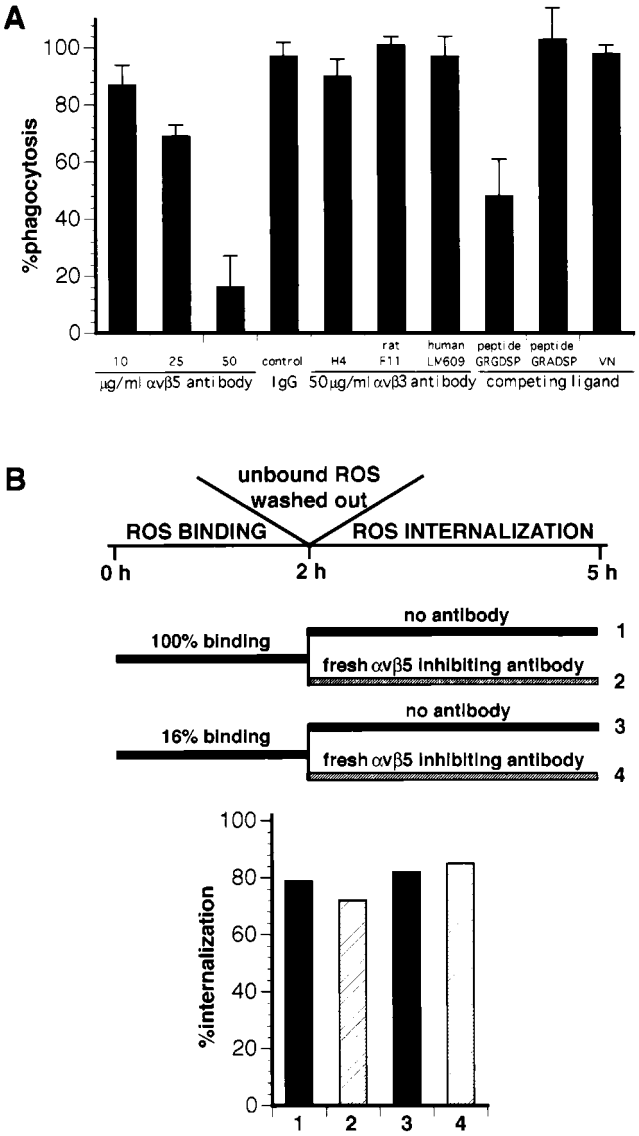

FIG. 5. ROS binding is inhibited by $\alpha v\beta 5$ antibody and by an RGD containing peptide but not by vitronectin. Internalization of surface-bound ROS is independent of $\alpha v\beta 5$ integrin. (*A*) Cells were challenged with FITC-ROS for 2 h after 30 min preincubation in the presence of the indicated reagents. Inhibition of phagocytosis by $\alpha v\beta 5$ antibody was concentration dependent, other antibodies did not alter ROS binding. Species-specific antibodies F11 (rat) and LM609 (human) were used solely on RPE-J or ARPE-19 cells, respectively. GRGDSP, but not a control peptide or vitronectin, competed with ROS binding. Phagocytosis of untreated samples represents 100%. Values are mean ± SD, $n = 8$, using RPE-J cells or ARPE-19 cells. Inhibition values were identical for both cell lines. (*B*) To determine the effect of $\alpha v\beta 5$ inhibition on ROS uptake, RPE cells were challenged with FITC-ROS in the absence (1, 2) or presence (3, 4) of $\alpha v\beta 5$ blocking antibody for 2 h; at this time, unbound ROS were washed out. Uptake of prebound ROS during the following three hours was in the presence (2, 4, ▨) or absence (1, 3, ■) of freshly added $\alpha v\beta 5$ blocking antibody. The flowchart outlines the treatment of different samples. For each sample, total fluorescence was measured after 5 h, then extracellular fluorescence quenched with trypan blue and the sample rescanned to measure the internalized fraction. The internalized fluorescence is given as percent of the total fluorescence of the sample at 5 h. Note that the total uptake at 2 h for samples 3 and 4 is 16% of the uptake by samples 1 and 2. Values represent mean values of two experimental sets; $n = 4$ for each sample in each experiment.

of ROS exposure; on the other hand, addition of antibody after 2 h did not alter the fate of RPE-bound ROS. Unlike other receptors that have been suggested to participate in later steps

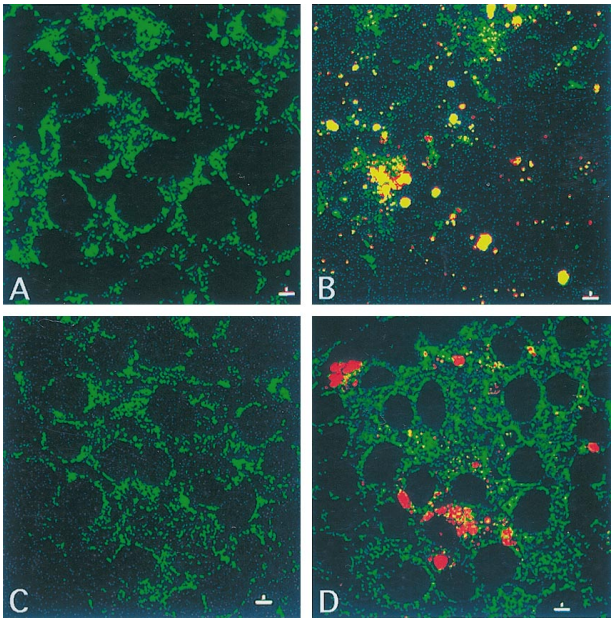

FIG. 6. $\beta 5$ integrin (but not $\beta 3$ integrin) codistributes with internalized ROS. Confocal microscopy sections of RPE-J cells reveal diffuse localization of $\beta 5$ and $\beta 3$ integrin when not challenged with ROS (*A*, $\beta 5$, and *C*, $\beta 3$). After phagocytosis of Texas red-labeled ROS for 5 h, $\beta 5$ integrin colocalized with phagocytosed ROS, appearing yellow (*B*). In contrast, in similar samples $\beta 3$ integrin and ROS derived fluorescence were distinct and the $\beta 3$ distribution pattern was unaltered (*D*). Bars = 5 μm.

of ROS phagocytosis (16, 17), $\alpha v\beta 5$ is the first RPE surface receptor necessary for binding but not for internalization of ROS.

Monocyte-derived macrophages utilize $\alpha v\beta 3$ and CD36, bridged by soluble thrombospondin, as coreceptors for phagocytosis of apoptotic cells (13). A similar situation may exist in RPE cells: $\alpha v\beta 5$ may cooperate with CD36 in the uptake of ROS. Thrombospondin is presumably present in the subretinal space (19), but it is currently not known whether thrombospondin or an alternative RPE counterpart is involved in ROS phagocytosis. Alternatively, $\alpha v\beta 5$ may act independently of other phagocytic receptors. The large inhibition of phagocytosis by $\alpha v\beta 5$ (Figs. 4 and 5) indicates that $\alpha v\beta 5$ integrin is the predominant receptor for ROS binding in RPE cells. The remaining 16% ROS uptake in the presence of $\alpha v\beta 5$ antibodies may be explained by a pool of recycling $\alpha v\beta 5$ that cannot be blocked by antibody, or by additional RPE receptor(s) playing a minor role. Additional experiments are needed to determine how many RPE receptors interact during ROS phagocytosis.

We observed that $\alpha v\beta 5$ integrin receptor dramatically relocalized with phagocytosis to the site of internalized ROS. That such removal of binding receptors from the RPE surface may downregulate phagocytosis at the end of their daily burst of activity is an interesting possibility that requires further studies.

RPE phagocytosis shows a remarkable specificity toward ROS (11) and $\alpha v\beta 5$ integrin is the first receptor exclusive to the RPE phagocytic mechanism (34, 35). Our results are consistent with a role for $\alpha v\beta 5$ in specific recognition of ROS by RPE cells. Since this recognition is inhibited by RGD containing peptides but not by vitronectin (Fig. 6), $\alpha v\beta 5$ may recognize a novel ligand on the surface of ROS. Its identification remains a challenge for future experiments.

We are grateful to the investigators who generously provided antibodies used in this study. This work was supported by the Dyson Foundation, National Institutes of Health Grant RO1 EY08538 and an RPB award to E.R.B., research fellowship FI-650 3/1 by the Deutsche

Forschungsgemeinschaft to S.C.F, and National Institutes of Health Grant F32 EY06669 (to A.D.M.). V.L.B. was supported by the Macular Degeneration Foundation.

1. Bok, D. (1993) *J. Cell Sci.* **17** (Suppl.), 189–195.
2. Young, R. W. & Bok, D. (1969) *J. Cell Biol.* **42,** 392–403.
3. Bok, D. & Hall, M. O. (1971) *J. Cell Biol.* **49,** 664–682.
4. Philp, N. J. & Bernstein, M. H. (1981) *Exp. Eye Res.* **33,** 47–53.
5. Ratto, G., Robinson, D., Yan, B. & McNaughton, P. (1991) *Nature (London)* **351,** 654–657.
6. Dowling, J. E. & Sidman, R. L. (1962) *J. Cell Biol.* **14,** 73–109.
7. Edwards, R. & Szamier, R. (1977) *Science* **197,** 1001–1003.
8. Mullen, R. J. & LaVail, M. M. (1976) *Science* **192,** 799–801.
9. LaVail, M. M., White, M. P., Gorrin, G. M., Yasumura, D., Porrello, K. V. & Mullen, R. J. (1993) *J. Comp. Neurol.* **333,** 168–181.
10. LaVail, M. M. (1976) *Science* **194,** 1071.
11. Mayerson, P. L. & Hall, M. O. (1986) *J. Cell Biol.* **103,** 299–308.
12. Savill, J., Dransfield, I., Hogg, N. & Haslett, C. (1990) *Nature (London)* **343,** 170–173.
13. Savill, J., Hogg, N., Ren, Y. & Haslett, C. (1992) *J. Clin. Invest.* **90,** 1513–1522.
14. Fadok, V. A., Savill, J. S., Haslett, C., Bratton, D. L., Doherty, D. E., Campbell, P. A. & Henson, P. M. (1992) *J. Immunol.* **149,** 4029–4035.
15. Lutz, D. A., Guo, Y. & McLaughlin, B. J. (1995) *Exp. Eye Res.* **61,** 487–493.
16. Boyle, D., Tien, L. F., Cooper, N. G., Shepherd, V. & McLaughlin, B. J. (1991) *Invest. Ophthalmol. Vis. Sci.* **32,** 1464–1470.
17. Ryeom, S. W., Sparrow, J. R. & Silverstein, R. L. (1996) *J. Cell Sci.* **109,** 387–395.
18. Ryeom, S. W., Silverstein, R. L., Scotto, A. & Sparrow, J. R. (1996) *J. Biol. Chem.* **271,** 20536–20539.
19. Hall, M. O., Burgess, B. L., Abrams, T. A., Ershov, A. V. & Gregory, C. Y. (1996) *Exp. Eye Res.* **63,** 255–264.
20. Anderson, D. H., Johnson, L. V. & Hageman, G. S. (1995) *J. Comp. Neurol.* **360,** 1–16.
21. Helfrich, M. H., Nesbitt, S. A. & Horton, M. A. (1992) *J. Bone Miner. Res.* **7,** 345–351.
22. Cheresh, D. & Spiro, R. (1987) *J. Biol. Chem.* **262,** 17703–17711.
23. Wayner, E., Orlando, R. & Cheresh, D. (1991) *J. Cell Biol.* **113,** 919–929.
24. Nabi, I. R., Mathews, A. P., Cohen-Gould, L., Gundersen, D. & Rodriguez-Boulan, E. (1993) *J. Cell Sci.* **104,** 37–49.
25. Dunn, K. C., Aotaki-Keen, A. E., Putkey, F. R. & Hjelmeland, L. M. (1996) *Exp. Eye Res.* **62,** 155–169.
26. Marmorstein, A. D., Bonilha, V. L., Chiflet, S., Neill, J. M. & Rodriguez-Boulan, E. (1996) *J. Cell Sci.* **109,** 3025–3034.
27. Molday, R. S., Hicks, D. & Molday, L. (1987) *Invest. Ophthamol. Vis. Sci.* **28,** 50–61.
28. Hed, J. (1986) *Methods Enzymol.* **132,** 198–204.
29. Chaitin, M. H. & Hall, M. O. (1983) *Invest. Ophthalmol. Vis. Sci.* **24,** 812–820.
30. Finnemann, S., Kuhl, M., Otto, G. & Wedlich, D. (1995) *Mol. Cell. Biol.* **15,** 5082–5091.
31. Smith, J. W., Vestal, D. J., Irwin, S. V., Burke, T. A. & Cheresh, D. A. (1990) *J. Biol. Chem.* **265,** 11008–11013.
32. Friedlander, M., Brooks, P. C., Shaffer, R. W., Kincaid, C. M., Varner, J. A. & Cheresh, D. A. (1995) *Science* **270,** 1500–1502.
33. Lewis, J. M., Cheresh, D. A. & Schwartz, M. A. (1996) *J. Cell Biol.* **134,** 1323–1332.
34. Blystone, S. D., Lindberg, F. P., LaFlamme, S. E. & Brown, E. J. (1995) *J. Cell Biol.* **130,** 745–754.
35. Ren, Y., Silverstein, R. L., Allen, J. & Savill, J. (1995) *J. Exp. Med.* **181,** 1857–1862.